Hindawi
Geofluids
Volume 2022, Article ID 5720228, 13 pages
https://doi.org/10.1155/2022/5720228

WILEY | Hindawi

Research Article

Upper Bound Finite Element Limit Analysis of Pullout Characteristics of Normal-Stressed Circular Anchor Plate

Yibo Luo,[1] Bin Wei,[2] Dongliang Huang,[1] Guoshun Lv,[1] and Shihong Hu[1]

[1]*School of Civil Engineering, Central South University, Changsha, 410075 Hunan Province, China*
[2]*Shenzhen Integrated Transportation Design Research Institute Co., Ltd., Shenzhen, 518001 Guangdong Province, China*

Correspondence should be addressed to Shihong Hu; 174812153@csu.edu.cn

Received 14 April 2022; Revised 2 May 2022; Accepted 13 May 2022; Published 8 June 2022

Academic Editor: Hao Wu

In this paper, the pullout factor and failure mode of circular anchor plate at an inclined angle with the horizontal ground under the normal stress are studied with the method of the upper bound finite element limit analysis. The effects of soil cohesion, internal friction angle, anchor plate inclination angle, and embedded ratio on the pullout factor are investigated to reveal the evolution of fracture surface of the soil around anchor plate under limit state. It is noted that the analysis of variance is adopted to process a series of data related to pullout capacity for obtaining the expression of the anchor plate's pullout factor. The results show that the internal friction angle is the key factor determining the pullout characteristics of the anchor plate. Particularly, the effect of the inclination angle on pullout capacity is highly correlated to the internal friction angle. For $\varphi = 0^\circ$, failure zone around anchor plate is presented as localization plastic zone and pullout capacity is linearly related to soil cohesion. The effect of inclination angle on pullout resistance is less significant. For $\varphi \neq 0^\circ$, the failure mode around the anchor plate is developing into full failure zone extending from both sides of anchor plate to ground. It is clearly noted that angle between the failure surface and horizontal line is greatly affected by the inclination of the anchor plate. Moreover, the effect of the inclination angle on pullout factor increases with increasing internal friction angle, which should be considered in the evaluation of the pullout bearing characteristics of the inclined circular anchor plate.

1. Introduction

Anchor plates embedded in soil are extensively applied in power transmission tower foundation, retaining wall of slope and other engineering projects. It often provides pullout resistance for various structures dependent on soil property and soil weight. With growing energy demand, there are needs for more constructions of engineering structures like offshore wind power towers and offshore oil platforms, creating a great prospect of application for anchor plates [1–5].

Existing literature pay great attention to anchor plates paralleling to the horizontal line. A series of small-scale laboratory model tests and centrifuge tests [6–8] are carried out to reveal the influence of the size of the anchor plate, soil density, and anchor embedment depth on ultimate uplift capability of circular anchor plates. In order to study the failure mechanism of the anchor plate, the digital image correlation method (DIC) is exploited to monitor the displacement of the soil [2, 9]. Besides, a variety of methods, including of quasistatic [10], upper bound limit analysis [11], small or large strain deformation elastic-plastic finite element analysis [12, 13], and lower bound or upper bound finite element limit analysis [1, 14–17] are employed to determine the behavior of anchor plate in clay and sand.

Although anchor plate is embedded at an angle between its normal line and the horizontal line to provide greater pullout resistance, few studies report comparison analysis between inclined anchor plates and horizontal anchor plates. It is clearly seen in the model test results of Das and Puri [18], the finite element results suggested of Fahmy et al. [19] and the finite element limit analysis results of Merifield et al. [20] and Bhattacharya and Kumar [21] that the inclination of anchor plate has significant effect on the critical embedded ratio and pullout resistance of anchor plate both in sand and clay. The dynamic pullout resistance of inclined strip anchor plate is also examined by Choudhury and Subba

Rao [22] and Priyanka. Research of Bhattacharya [23] and Bhattacharya [24] studied how the influence of distance away from the sloping ground and the discreteness of soil strength affect the pullout resistance of anchor plates, respectively.

According to extant papers, it seems that few scholars have fitted the expression of the pullout factor of circular anchor plate taking into consideration the cohesion, friction angle, and the inclination of the anchor plate at the same time. It is a concern that the derivation of theoretical formula of the pullout factor expression is too difficult to be described in previous researches. However, the method of fitting the expression of material strength and material composition in the material field [25, 26] shows that the data analysis methods can determine the effect of related factors and the form of expression when reliable data is available.

In this paper, finite element limit analysis software Optum G3 is used to obtain the pullout factor and failure mechanism of the normal-stressed circular anchor plate whose normal line is inclining at θ relative to the horizontal line. For simple condition such as $c = 0$ kPa or $\varphi = 0°$, the qualitative analysis based on graphics is used to investigate the influence of soil properties and the inclination angle on the pullout factor of anchor plate. For $c \neq 0$ kPa and $\varphi \neq 0°$, the quantitative analysis based on analysis of variance is used so as to decompose the influence of soil properties and the inclination angle into the main effects and interaction effects of soil cohesion, internal friction angle, anchor plate inclination angle, and embedded diameter ratio on the anchor plate's pullout factor. Since the results of qualitative analysis determined the influence of each parameter, and thereby, the expression of the pullout factor for inclined circular anchor plate is fitted with the solutions of Optum G3 in an attempt to assist engineering design. Besides, the effect of soil properties and the inclination angle on the failure surface is exclusively presented to evaluate the performance of pullout capacity of anchor plate.

2. Problem Definition

2.1. Pullout Factor of Plate Anchor. A circular anchor plate of diameter D is embedded in soil at depth H with an inclination θ in horizontal direction as shown in Figure 1, where γ is the unit weight of the soil, c is the cohesion of soil, φ is the internal friction angle of soil. P_u is the normal ultimate pullout resistance of anchor plate. The index of pullout factor is calculated as shown in Equation (1), where N_s is the pullout factor of anchor plate, and A is the area of the anchor plate.

$$N_s = \frac{P_u}{\gamma A H}. \tag{1}$$

2.2. Numerical Model. There are several basic principles of the upper bound finite element limit analysis whose finite element mathematical optimization model is shown in Equation (2) [27–29] as follows. Firstly, the finite element is used to discretize the velocity field of the soil mass. Secondly, the total internal energy dissipation of the soil mass is taken as the objective function, and the constraint equation (or inequality) that satisfies the kinematic admissible condition is established in the discrete velocity field; equivalently, the upper bound theorem is transformed into the corresponding mathematical programming problem. Finally, the established model is solved by the appropriate mathematical programming algorithm, and the velocity field under the limit state is searched by the computer. Finite element limit analysis exhibits great advantages in the academic and practical works. On the one hand, finite element limit analysis is superior to finite element analysis for its convenience in solving ultimate load and the failure mechanism without conducting analysis of the whole process of load-displacement-destruction, simplifying the solution process of the ultimate bearing capacity of the anchor plate. On the other hand, compared with the traditional limit analysis method, the finite element limit analysis overcomes the difficulty of constructing the kinematic admissible velocity field, which makes it appropriate to simulate the pullout process of the inclined circular anchor plate.

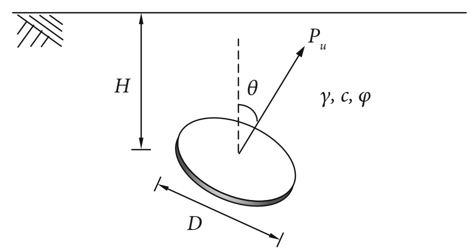

Figure 1: Problem geometry.

$$\begin{cases} \text{min}: & \sigma^T B u - c^T u \\ \text{subject to}: & Au = b \\ & Bu = \sum_{j\in J} \dot{\lambda}_j \nabla f_j(\sigma) \\ & \sum_{j\in J} \dot{\lambda}_j \nabla f_j(\sigma) = 0, j \in J \\ & \dot{\lambda}_j \geq 0, j \in J \\ & f_j(\sigma) \leq 0, j \in J \\ & u \in R^{n_u}, \sigma \in R^{n_u} \end{cases} \tag{2}$$

where σ represents the global stress column vector; B represents the global compatibility matrix; u represents the global velocity column vector; c represents the column vector of coefficients for a linear function of external force power; A and b are the coefficient matrix and right-hand term of the global linear constraint equation, respectively; λ represents plastic multiplier rate column vector; f_j is the plastic yield function of element stress; $\dot{\lambda}_j$ is the plastic multiplier rate corresponding to f_j; and J represents the set of all stress yield functions.

The finite element limit analysis software used in this paper is Optum G3, which incorporates limit analysis theory and finite element theory. Optum G3 has a series of methods to conduct the finite element limit analysis and complete built-in adaptive meshing function. This means that the grid can be automatically refined according to the failure mode, characterized by its improvement in grid utilization and calculation speed without decreasing calculation accuracy. In the research of Giampa et al. [1], Optum G2, two-dimensional versions of Optum G3, is employed to study the effect of dilation angle on the ultimate bearing capacity of anchor plate and proved to exhibit good applicability. Since the core theories of Optum G2 and Optum G3 remain the same, the research of Giampa et al. [1] also documents that Optum G3 is suitable for pullout analysis of anchor plates.

Generally, the weight of the anchor plate is assumed to be ignored compared to its ultimate pullout resistance. The rigidity of the anchor plate is much greater than that of the soil. The weightless rigid anchor plate is adopted in the paper. The soil is assumed to follow the Mohr-Coulomb failure criterion and an associated flow criterion. The boundary conditions satisfy width $W > H + D$ and length $L > 2H + D$, which is similar to that of Merifield et al. [15] and Choudhary et al. [30]. No energy dissipation in the boundary of domain presented in results indicates that the ultimate pullout resistance of the anchor plate is free from effects of boundary condition and adequate model domain set. The bottom boundary is fully constrained, and the side boundary is normally constrained. For anchor plate in cohesive soil, only the fully attached condition is considered to simulate the situation where suction maintains full contact between soil and anchor.

The type of finite element is upper bound elements and the maximum grid size and appropriate number of grid iterations are chosen to ensure that the mesh is free from irregular deformation and the pullout resistance of each iteration converges within 5%. In this way, grids meet the requirements of mechanical simulation behavior. Only half the model is simulated using symmetry to reduce computational efforts. The typical meshing result is shown in Figure 2. Based on the above numerical model, a series of numerical simulations are carried out using the MOSEK solver to study the effect of various parameters on the pullout capability of inclined circular anchor plates in soil. According to the research of Murray and Geddes [31], Merifield et al. [32], and Song et al. [33], the parameter values are selected as shown in Table 1. Parameters include soil cohesion (c), internal friction angle (φ), depth ratio of anchor plate (H/D), and inclination (θ). The value range of soil cohesion, friction angle within the soil, and anchor plate inclination are 0-40 kPa, 0-40°, and 0-90° in turn, with the interval of 10 kPa, 10°, and 15° in turn. The value of embedded ratio is taken from 1-8 in turn. Totally, the pullout factors of the anchor plate under 1400 $(5 \times 5 \times 7 \times 8)$ parameter combinations are calculated in this paper.

2.3. Model Comparison. Before the discussion of pullout capacity of the anchor plate, it is necessary to ascertain the accuracy and validity of numerical model. For $c = 0$ kPa, the current numerical simulation results are compared with those results obtained by the method of limit analysis [31, 34] and limit equilibrium [35] as shown in Figure 3(a). Although the current results are lower than that of the limit equilibrium solutions, the comparison demonstrates that the current results are similar to both limit analysis solutions, with a relative error of less than 5%.

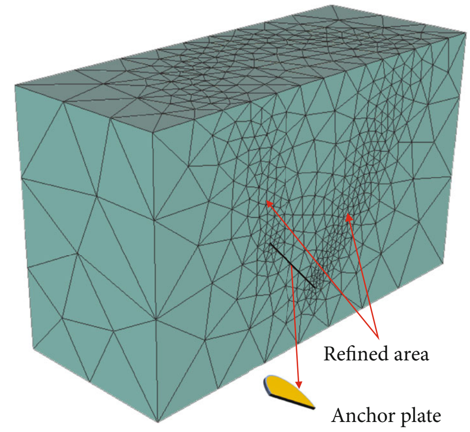

Figure 2: Mesh details of model.

For $\varphi = 0°$, as shown in the comparison between the current numerical simulation results and existing finite element limit analysis results [32] and finite element results [33, 36] shown in Figure 3(b), the gap of relative errors between the current results and the result of Song et al. [33] is less than 5%. Meanwhile, if $H/D \geq 3$, the overall trends of these results are similar. The difference between the result of Song et al. [33] and Wang et al. [36] is caused by the different value of E/c, which is not required in the finite element limit analysis but has a great effect on the critical embedded ratio of anchor plate in the finite element limit analysis. Their researches have both extensively detailed the effect of E/c, indicating that the critical embedded ratio of anchor plate will be larger in the soil with larger value of E/c. However, difference between the result of the current study and the result of Merifield et al. [32] occurs due to different breakaway conditions. The anchor plate is fully attached in this paper, whereas it is an immediate breakaway in the study of Merifield et al. [32]. Compared with the fully attached condition, the anchor plate in immediate breakaway state generally has a larger critical embedded ratio and lower pullout resistance [33, 36]. To sum up, the resemblance between results reported in previous studies and results obtained in the paper validates that our model design is strongly convincing.

3. Results and Analysis

After verifying the accuracy of the limit analysis model, our study conducts a qualitative discussion of how anchor plate's pullout factor adjusts to different soil cohesions, internal friction angles, anchor plate inclinations, and embedment depths. Then, based on the theory of variance analysis, the effects of parameters on anchor plate's pullout factor are quantitatively discussed. Besides, the method of fitted regression is applied in the expression in terms of pullout factor of the normally stressed circular inclined anchor plate.

3.1. Effect of Strength of Soil on N_s. Figure 4 shows the pullout factor of anchor plates at different inclination angles for $c = 0$ kPa, $H/D = 2$ and $c = 0$ kPa, $H/D = 4$. It is found that

Table 1: Properties of numerical model.

Diameter of plate anchor D (m)	Unit weight of the soil γ (kN/m^3)	Cohesion c (kPa)	Friction angle φ (°)	Embedment ratio (H/D)	Inclined angle of plate anchor θ (°)
1	20	0-40	0-40	1-8	0-90

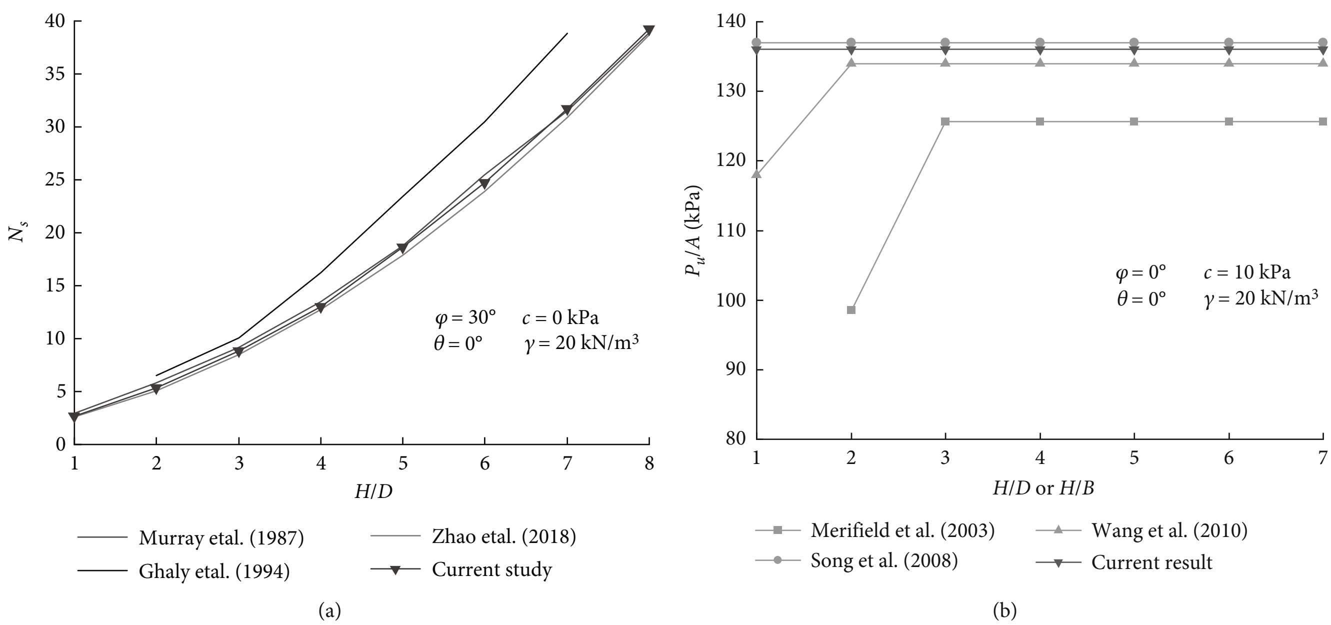

Figure 3: Variation and comparison of pullout capacity with available data in existing literature for anchor plate at different H/D for (a) $c = 0$ kPa and (b) $\varphi = 0°$.

the pullout factor of anchor plate is positively correlated with anchor plate's inclination angle and soil's friction angle. The larger the internal friction angle becomes, the more significant effect of anchor plate's inclination angle on the pullout factor. The pullout factor increases significantly with the increasing inclination angle in the case of inclination angle $\theta > 45°$. The pullout factor of the anchor plate with varying inclination angles is shown in Figure 5 for $\varphi = 0°$ and $H/D = 4$. Figure 5(a) plots minor changes of the pullout factor of the anchor plate with different inclination angles of anchor plates, and Figure 5(b) illustrates that the pullout factor of the anchor plate linearly increases with the increase in cohesion shown. It is thereby proven that the effect of the anchor plate's inclination angle on the pullout factor is more significant, when the internal friction angle increases. In the case of the internal friction angle $\varphi = 0°$, the soil cohesion is a decisive parameter for the anchor plate's pullout factor, and the inclination angle has marginal effect on anchor plate's pullout factor.

3.2. Effect of Embedment Ratio on N_s. The magnitudes of pullout factors affected by the inclination angle at different embedment depths are shown in Figure 6. It is observed that pullout factor of the anchor plate increases with the increase in both the embedment ratio and the inclination of the anchor plate in loose sand. The anchor plate's inclination exerts greater effect on pullout factors of anchor plates at relatively deeper embedment ratio. For the anchor plate in clay, the magnitude of pullout factor is negatively correlated with the increase of the embedment ratio, while the effect of inclination of the anchor plate seems to be the same under different embedment ratios. It is noteworthy that the pullout factor decreases with the increase in anchor plate's inclination angle at embedment ratio $H/D = 1$, indicating that the effect of inclination of anchor plate in clay on pullout factor is assumed to be negligible when embedment depth ratio is greater than critical value. Therefore, the effect of the embedment ratio on pullout factor of the anchor plate is influenced by soil properties and the inclination angle of anchor plate.

3.3. Analysis of Variance on N_s. For $c > 0$ kPa and $\varphi > 0°$, the pullout resistance of the inclined anchor plate is affected by a variety of factors, including soil cohesion, internal friction angle, anchor plate inclination angle, and buried diameter ratio, which is essentially a multi-independent variable problem. A line chart is unable to satisfy the requirements in solving multi-independent variable problem because it can only explore the main effect of each variable determined by its own level on the dependent variable. In the multi-independent variable problem, the effect of the independent variable on the dependent variable is usually determined by

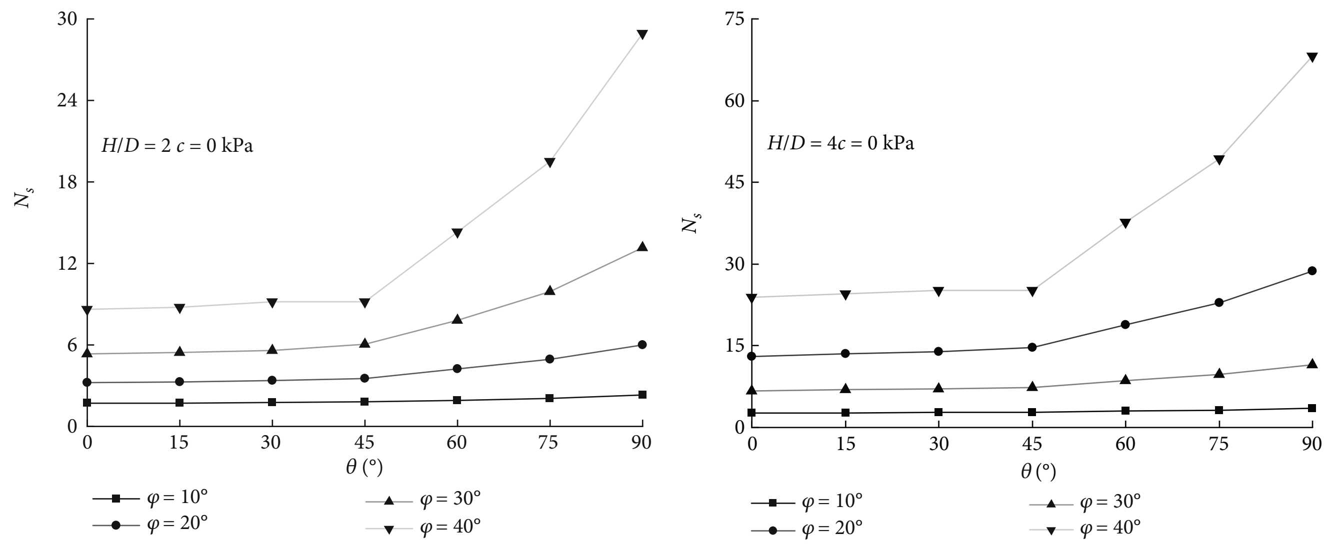

(a) (b)

Figure 4: N_s of circular plate anchor at different inclination angles for $c = 0$ kPa.

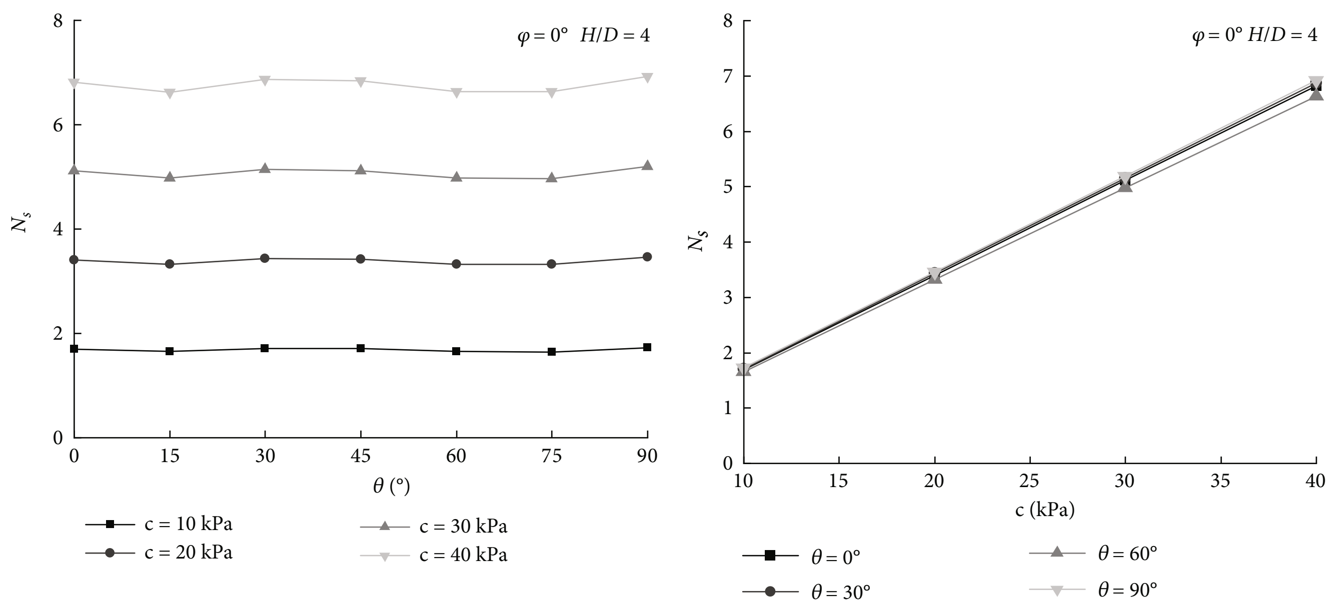

(a) (b)

Figure 5: N_s of circular plate anchor at different inclination angles for $\varphi = 0^\circ$.

independent variable itself and the interactive effect between different independent variables. In addition, graphs depicted above have no quantitative implications for how significant the effect of independent variables exert on the decisive influence factors. In order to overcome this dilemma, analysis of variance method is proposed by Fisher [37]. This method enables the variance of the dependent variable to be attributed to the variance of independent variable and the variance of interaction between independent variables. The sensitivity of the dependent variable to the factor is determined by the variance associated with the factor. Since the method of analysis of variance has been widely used in various fields, such as fitting the expression of material strength and material composition in the material field [25, 26], this paper employs the analysis of variance method to quantify the influence of various parameters on the pullout factor of the anchor plate for $c > 0$ kPa and $\varphi > 0^\circ$.

Analysis of variance is a probabilistic method, and the accuracy of its results depends on the reliability of the sample. The research proposed by [38] shows that the adoption of analysis of variance requires sample data to meet the following assumptions: (1) the sample data are mutually

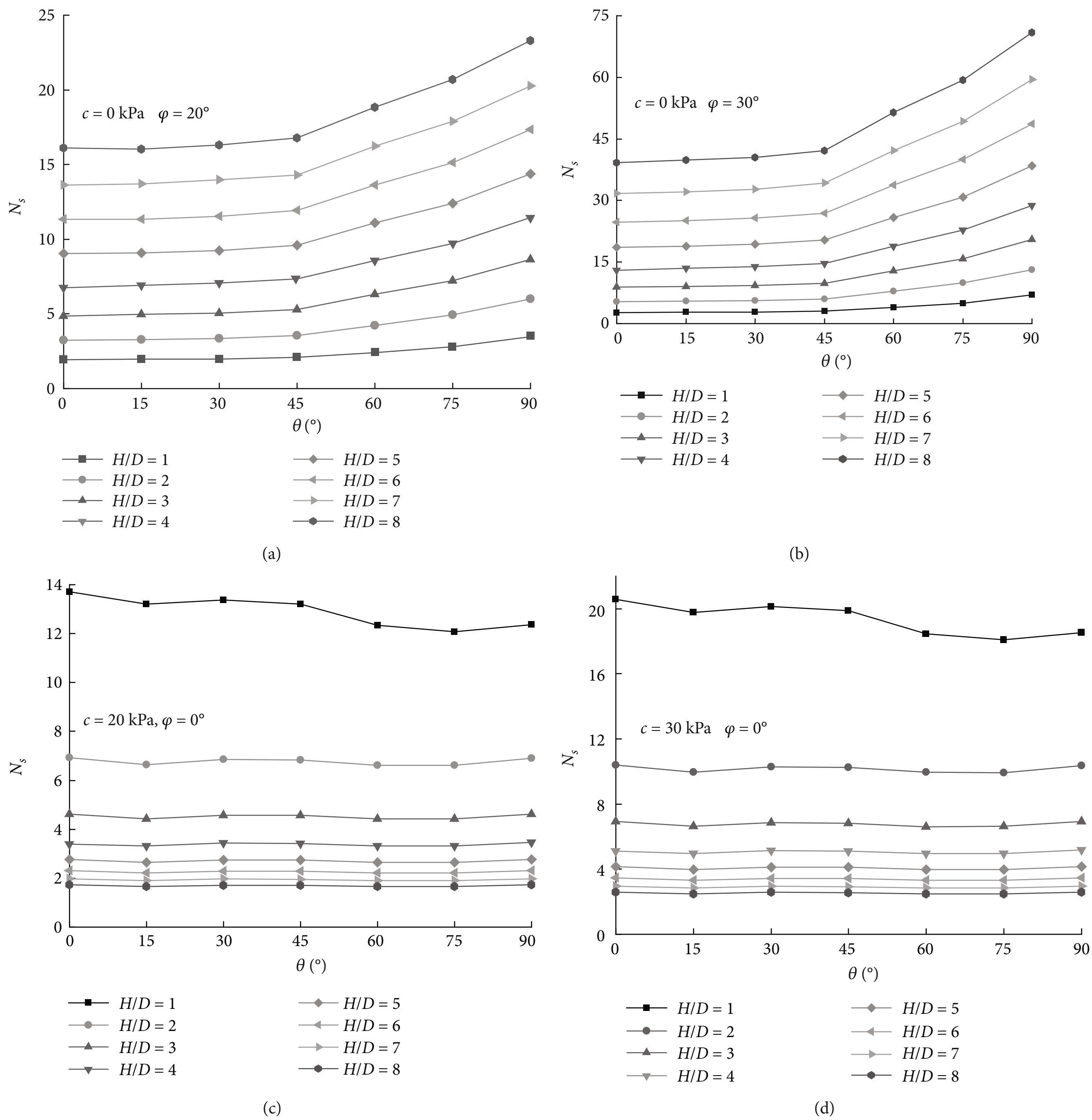

FIGURE 6: N_s of circular plate anchor at different H/D for $c = 0$ kPa and $\varphi = 0°$.

independent; (2) the sample data obey the normal distribution; and (3) the sample errors are consistent. In this paper, the limit analysis finite element method is used to estimate the pullout resistance of the anchor plate with different parameters. The requirements of (1) and (3) are met by building an accurate model. The research of Blanca et al. [39] suggests that the analysis of variance method is highly applicable. The sample that does not obey the normal distribution can still be applied in the analysis of variance method and clarify the correlation between the independent variable and the dependent variable. Then, the pullout factor can be directly used in the analysis of variance without standard normalization.

After data processing, a general linearization model shown in Equation (3) is used to illustrate the effect of various factors on the pullout factor of the anchor plate. The applicability of the model will be discussed in the subsequent sections. In Equation (3), N_{ijkl} represent the pullout factor for cohesion, internal friction angle, anchor plate inclination angle, and embedment ratio with the value of c_i, φ_j, θ_k, and

η_l, respectively. The indices i, j, k, and l represent different values of cohesion, internal friction angle, anchor plate inclination angle, and embedment ratio. α_{ij}, β_{ik}, λ_{il}, τ_{jk}, υ_{jl}, and ω_{kl} represent the increment of different interactions of factor. For example, α_{ij} represents that the increment is merely caused by the interaction effect of cohesion c_i and internal friction angle φ_j. ε_{ijkl} denotes the model error and represents the effect of other factors that are neglected in this model on the pullout factor of the anchor plate. It should be noted that Equation (3) is an abstract mathematical model rather than a specific calculation expression. Equation (3) characterizes that the pullout capacity of the anchor plate is the summation of the influence of parameters such as cohesion and internal friction angle and their interactive effect, instead of saying that the pullout capacity is regarded as the simple sum of the values of each parameter.

$$N_{ijkl} = \mu + c_i + \varphi_j + \theta_k + \eta_l + \alpha_{ij} + \beta_{ik} + \lambda_{il} + \tau_{jk} + \upsilon_{jl} + \omega_{kl} + \varepsilon_{ijkl}. \quad (3)$$

In order to fully analyze the interaction effect between parameters on the pullout factor of anchor plate, 896 sets of data calculated by Optum G3 for $c \neq 0\,\text{kPa}$ and $\varphi \neq 0°$ are selected as the sample data for the analysis of variance. The confidence level is set as 95% and the coefficient of determination of the model is 0.989, implying that the model shown in Equation (3) demonstrates 98.9% of the change of the pullout capacity at the 95% confidence level. In other words, Equation (3) fits the sample data well and a linear relationship exists between the effects of various parameters mentioned in Equation (3) and the pullout capacity of the anchor plate. Meanwhile, the high goodness of fit of the model also indicates that interactions higher than the second order have less influence on the pullout capacity of the anchor plate. Interactions higher than the second order among parameters can be ignored in the design.

The F-factors of each factor obtained from the analysis of variance are shown in Figure 7, and the complete analysis of variance table is shown in Table 2. According to the principle of analysis of variance, the larger the F-factor value, the stronger the sensitivity of the anchor plate pullout capacity to this factor.

The F -factors for interactions between parameters shown as Figure 7(b) are smaller than that of parameters' first-order effects shown as Figure 7(a), suggesting that the first-order effects of parameters are mainly responsible for the pullout capacity. In Figure 7(a), the F -factors for soil's internal friction angle and anchor plate's embedment ratio are bigger than F-factors for other parameters, which indicates that the internal friction angle and the embedded ratio of the soil are the main parameters affecting anchor plate's pullout capacity. It can be noted in Figure 7(b), that the F -factors for interactions between the anchor plate inclination angle and the embedment ratio, the interaction between the cohesion and the inclination angle of anchor plate, and the interaction between the cohesion and the embedment ratio are much smaller than the F -factors for the other interactions. Additionally, the effect of cohesion on the pullout capacity of anchor plate is hardly affected by the inclination angle and the embedment depth of the anchor plate as shown in Figures 5 and 6 and the effect of the inclination angle of the anchor plate is hardly affected by the embedment diameter ratio of anchor plate as shown in Figures 4 and 6. The result of analysis of variance has a good agreement with quantitative researches conducted by Ilamparuthi et al. [7] and Al Hakeem and Aubeny [12] and therefore exhibits strong validity of the analysis of variance. Furthermore, as shown in Figure 7(b), the F -factor of the interaction between the internal friction angle of soil and other parameters should be considered. It is found that the interactions term between inclination angle and cohesion, interaction term between inclination and inclination angle, and interaction term between inclination angle and embedment ratio, respectively, exert significant influence on the pullout factor of anchor plates.

3.4. Linear Regression of N_s. The basic principles for determining the expression of the anchor plate's pullout factor by means of data analysis are as follows: firstly, the analysis of variance is used to identify factors that have a significant effect on the pullout factor of the anchor plate; secondly, the influence form of each factor (exponential, logarithmic, or other types) is determined based on the qualitative analysis of the effect of each factor on the pullout factor for $c = 0\,\text{kPa}$ and $\varphi = 0°$; and finally, multiple fitting expressions with reference to the existing fitting formula are determined and the expression with the best goodness of fit is selected. Based on this process, this paper finally determines the expression shown in Equation (4) as the expression of the anchor plate pullout coefficient for $c \neq 0\,\text{kPa}$ and $\varphi \neq 0°$. The coefficients in Equation (4) are estimated and obtained based on numerical simulation as shown in Table 3.

It is noted that (a) for the case of $\theta \leq 45°$, the model demonstrates 97.74% of the variation of the pullout factor; (b) for the case of $\theta > 45°$, the model reflects 97.33% of the variation of the pullout factor. Therefore, the expression is appliable for fitting the anchor plate's pullout factor under the impact of different parameters. The estimation results in Table 3 indicate that the coefficients of Equation (4) display a large disparity between the case of $\theta \leq 45°$ and $\varphi > 45°$. It is noted that the effect of the inclination angle on the pullout factor of the anchor plate shows discrepancy with 45° as a dividing line. It is logic to deal with the coefficients of Equation (4) by using the piecewise fitting method.

As shown in Figure 8, for $\varphi \neq 0°$, changing the value of cohesion will not significantly affect the failure mechanism of the anchor plate which indicates that the change of soil cohesion does not significantly change the influence of other factors. Therefore, Equation (4) is suitable for calculating the pullout factor for $c = 0\,\text{kPa}$ and $\varphi \neq 0°$ if the value of cohesion is set to 0 kPa. However, as shown in Figures 5(a) and 6(b), the effect of the inclination angle and embedded ratio of the anchor plate on the pullout factor is almost negligible. Consistent to the study of Song et al. [33], the critical embedded ratio of the fully attached anchor plate studied in this paper is less than 1. Given that the failure mechanism

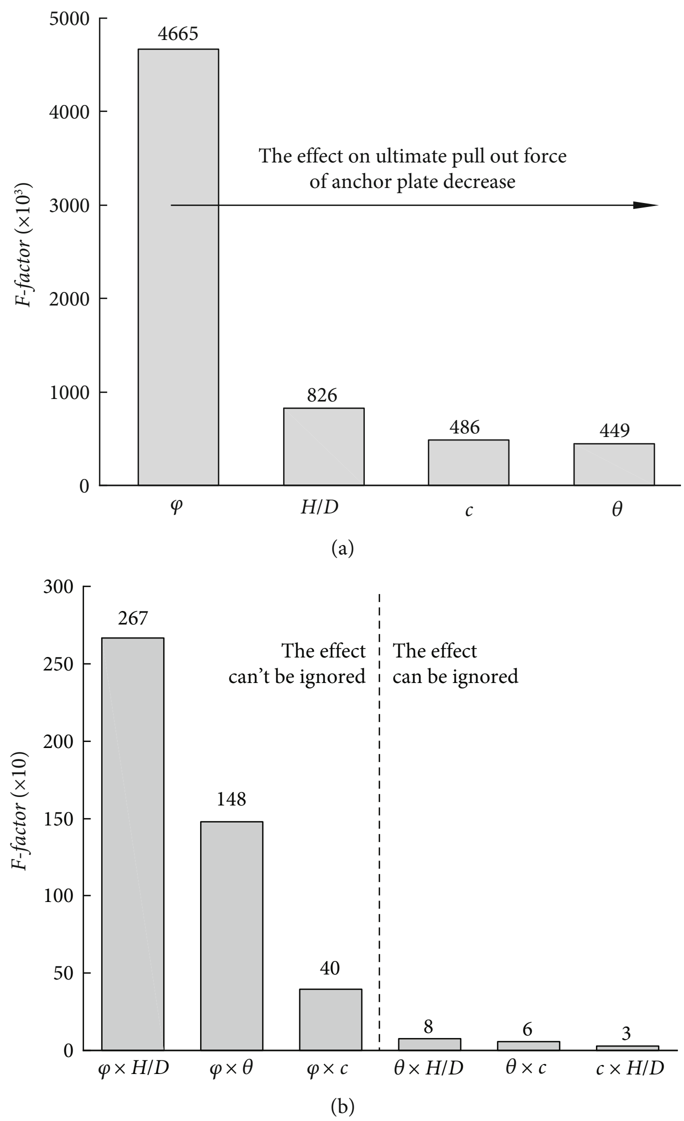

Figure 7: The F-factor of each factor's (a) main effect and (b) interaction effect.

Table 2: ANOVA table of N_s for cohesion, friction angle, inclined angle and embedment ratio(R^2=0.989).

Source of variation	*SS*	*df*	*MS*	*F-factor*	*Sig. F*
Model	3260883.475	148	22032.993	436.091	.000
Inclined angle(θ)	136070.845	6	22678.474	448.790	.000
Cohesion(c)	73733.474	3	24577.825	486.377	.000
Embedment ratio(H/D)	292222.273	7	41746.039	**826.124**	.000
Friction angle(φ)	707138.823	3	235712.941	**4664.587**	.000
Interaction of c and H/D	2933.719	21	139.701	2.765	.000
Interaction of c and θ	5027.840	18	279.324	5.528	.000
Interaction of θ and H/D	16611.465	42	395.511	7.827	.000
Interaction between c and φ	18020.884	9	2002.320	39.624	.000
Interaction of φ and θ	134499.253	18	7472.181	147.869	.000
Interaction of φ and H/D	283062.901	21	13479.186	266.743	.000
Error of estimate	37747.731	747	50.532		
Total	3298631.206	895			

Table 3: Value of regression coefficient.

Inclination angle (θ)	k_1	k_2	k_3	k_4	k_5	k_6	R^2
≤45°	13.2	-55.49	0.33	19.96	22.52	18.4	0.9774
>45°	13.2	-183.10	-0.80	177.49	34.85	31.2	0.9733

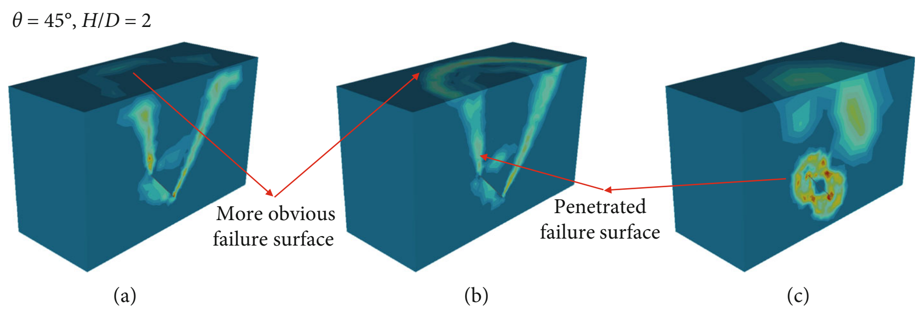

Figure 8: 3D-Failure of circular anchor plate in (a) loose sand, (b) normal soil, and (c) pure clay.

of the anchor plate for $\varphi = 0°$ is obviously different from the anchor plate for $\varphi \neq 0°$, Equation (4) is not suitable for calculating the pullout factor of the anchor plate in fully clay. According to Figure 5(b), the pullout factor of the anchor plate for $\varphi = 0°$ is proportional to the cohesion of soil. Therefore, Equation (5) is selected as the expression of the pullout factor of the anchor plate for $\varphi = 0°$. In Equation (5), k_7 is a dimensionless coefficient, which characterizes the positive correlation between the pullout factor of the anchor plate and the cohesion of the soil. The results of numerical simulation for $\varphi = 0°$ are used to fit the coefficients in Equation (5) and the result shows that k_7 equals 13.6 in agreement with the results of Song et al. [33] and Wang et al. [36], i.e., 13.7 and 13.4, respectively.

$$N_s = k_1 \frac{c}{\gamma H} + k_2 \tan^2\varphi + k_3 \frac{H}{D} + k_4 \tan^2\varphi \tan(\theta/2) + k_5 \frac{H}{D} \tan^2\varphi + k_6 \frac{c}{\gamma D} \tan^2\varphi, \quad (4)$$

$$N_s = k_7 \frac{c}{\gamma H}\,; \varphi = 0°, H/D \geq 1. \quad (5)$$

Comparisons between estimation results and numerical simulation solutions for different parameter levels are shown in Figure 9. The points in Figure 9 are the results obtained by using limit analysis finite element (FELA), and the solid line represents the results of regression analysis (RE). The numerical simulation results distributed on the curves indicate that the effect of the inclination angle on pullout factor of anchor plate is correctly estimated by regression analysis. In Figures 9(a), 9(b), and 9(c), respectively, it is shown that Equation (4) and Equation (5) better capture the effect of cohesion, internal friction angle, and embedment ratio of anchor plate on the pullout factor.

3.5. Failure Surface in Sand. Figure 10 shows the displacement field of the soil when the anchor plate reaches its ultimate pullout capacity in loose sand. It is seen that the displacement field around the horizontal anchor plate is symmetrically distributed, and symmetrical linear shear bands exist at both sides of the anchor plate. However, the shear bands of the inclined anchor plate are asymmetrically distributed. The researches presented by Liu et al. [9] and Choudhary et al. [30] based on model tests and numerical model, respectively, present the fracture surface of the horizontal anchor plate in sand as shown in Figure 10(a). The shear dissipation mode with 1/2 section of the anchor plate is shown in Figure 11. The following is noted:

(a) For $\theta < 45°$, the failure surfaces on both sides of the anchor plate are linear. The angle between the left failure surface and the horizontal direction increases with the increase in the inclination angle of the anchor plate, the angle between the right failure surface and the horizontal direction is almost constant

(b) For $\theta > 45°$, the left fracture surface of the anchor plate is presented as a straight line and the intersection angle with the horizontal direction is almost unchanged, the right fracture surface gradually witnesses a change from a straight line into a curve with the inclination angle increases. Meanwhile, the angle between the bottom of right fracture surface and the horizontal direction gradually decreases. In addition, for the inclination angle $\theta > 45°$, a shear dissipation zone enveloping the interior of the soil appears above the anchor plate. This reflects that the soil energy dissipation increases

The results show that the fracture surface on the right side of the anchor plate is influenced by inclination angle of the anchor plate, and shear stress of the soil above the anchor plate is positively associated with the inclination angle of the anchor plate.

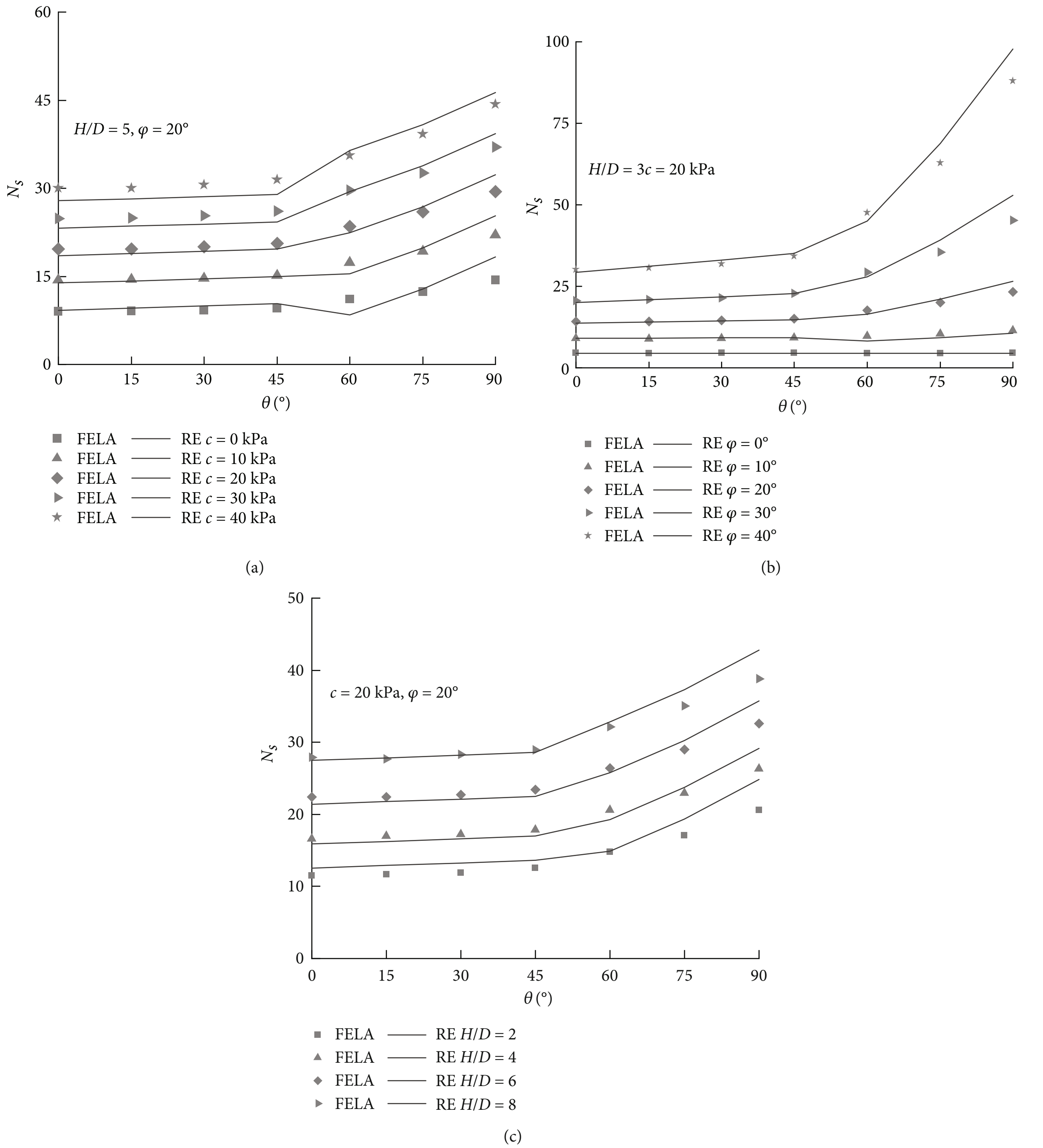

Figure 9: Comparison of numerical simulation results and regression results for different (a) cohesion, (b) internal friction angle, and (c) H/D.

3.6. Failure Surface in Clay. Figure 12 shows the soil displacement when the anchor plate in clay bears the ultimate pullout capacity. It is clearly seen that an elliptical plastic zone with the anchor plate as the axis of symmetry is formed inside the soil with varying inclination angle of anchor plate. When the inclination of anchor plate changes, marginal difference occurs in the shape of plastic zone, and the zone develops with the rotation of the anchor plate. This is similar to the fracture surface in the research proposed by Fahmy et al. [19] on strip anchor plates in clay. The results show that similar soil shear dissipation mode is the reason why the effect of the inclination angle on the pullout factor of the anchor plate is almost negligible for the internal friction angle $\varphi \neq 0°$.

3.7. Effect of Soil Strength on Failure Surface. Figure 8 illustrates the shear dissipation mode when the anchor plate reaches the ultimate bearing capacity in loose sand, general

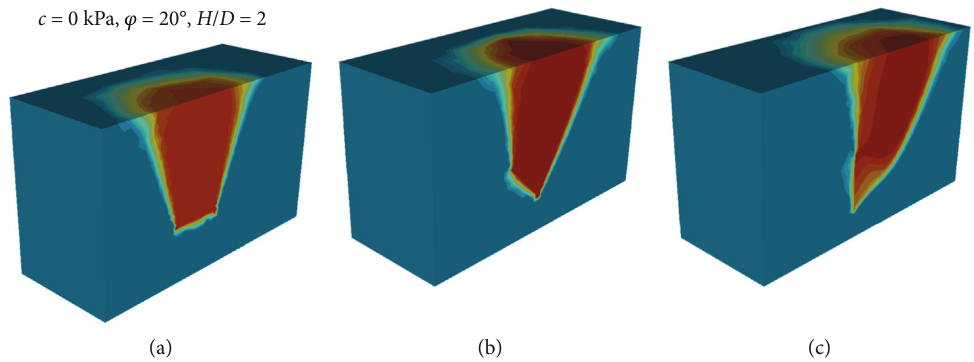

Figure 10: 3D-Failure of circular anchor plate at (a) $\theta = 0^\circ$, (b) $\theta = 45^\circ$, and (c) $\theta = 90^\circ$ for $c = 0$ kPa.

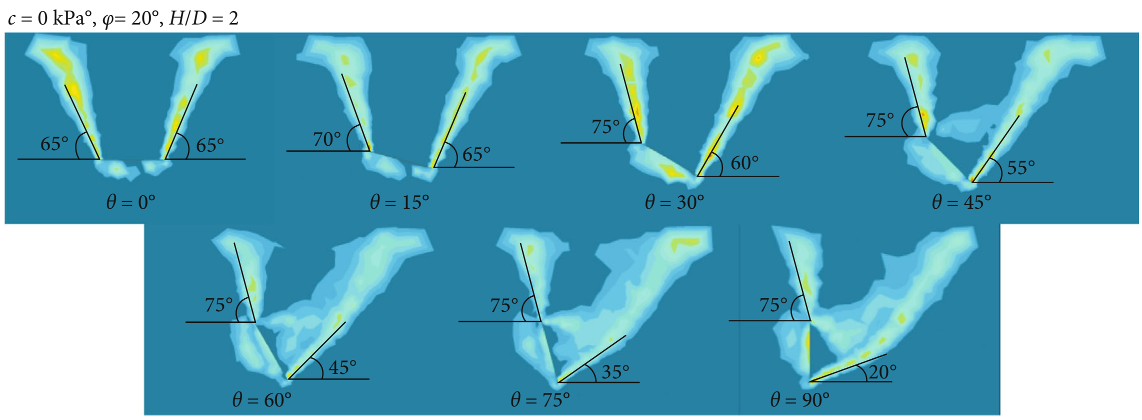

Figure 11: Shear dissipation of circular anchor plate for loose sand at different θ.

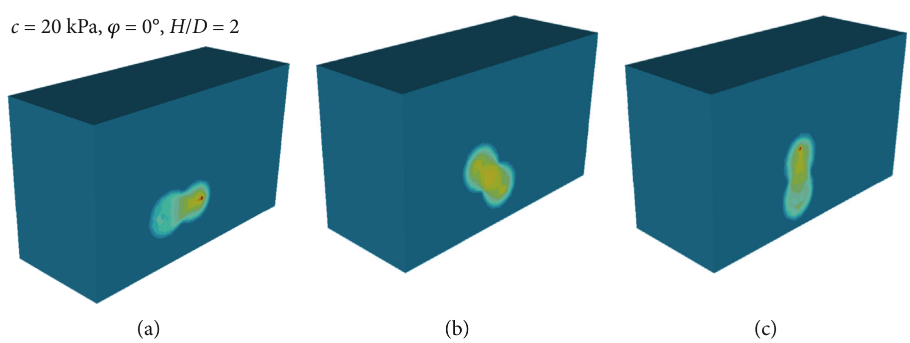

Figure 12: 3D-Failure surface of circular anchor plate at (a) $\theta = 0^\circ$, (b) $\theta = 45^\circ$, and (c) $\theta = 90^\circ$ for $\varphi = 0^\circ$.

soil, and pure clay. From comparison of Figures 8(a) and 8(b), it is noted that the shear dissipation energy of soil on both sides of the anchor plate increases with the increase in cohesion, and a more obvious shear dissipation zone occurs on the surface of the soil. Comparison between Figures 8(b) and 8(c) indicates that changes of the internal friction angle in soil affected failure mode of the soil significantly. On the one hand, variations of soil's internal friction angle have a significant influence on the failure mode and thereby the ultimate uplift load of the anchor plate being the reason why the internal friction angle of soil significantly affects the pullout factor of the anchor plate. On the other hand, the energy dissipation of the soil extends up with the increase in cohesion. In other words, both the power dissipation of the soil and pullout factor of the anchor plate increase.

4. Conclusion

In the paper, based on the limit analysis finite element method, a battery of numerical analysis are conducted to examine the effect of influencing parameters such as cohesion, internal friction angle, anchor plate inclination, and buried depth on the pullout capacity of the normal-stressed circular anchor plate. Besides, regression analyses are applied to obtain the calculation expression in term of the pullout factor of the inclined circular anchor plate. Conclusions are drawn as follows:

(1) The parametric study shows that cohesion, internal friction angle, anchor plate inclination, and embedding ratio all have positive effects on pullout factor of anchor plate

(2) The analysis of variance shows that parameters with respect to the significance of their effects on the pullout capacity rank as follows: internal friction angle with the biggest influence, embedment ratio followed, then cohesion, and anchor plate inclination with the weakest influence

(3) For anchor plate in sand, the shear dissipation band on the left side of anchor plate is almost unchanged while the shear dissipation band on the right side gradually changes from linear to nonlinear as the inclination angle increases

(4) For anchor plate in clay, the contours of shear dissipation zone are local and confined within soil in the shape of ellipsoid. With the change of inclination of anchor plate, the shear dissipation zone is always distributed with the anchor plate as the symmetry plane

Data Availability

All the data, models, or codes that support the findings of this study are available from the corresponding author upon reasonable request.

Conflicts of Interest

The authors declare that they have no conflicts of interest.

Authors' Contributions

All authors make contributions to the study conception and design. Data collection and analysis were performed by Yibo Luo, Bin Wei, Dongliang Huang, Guoshun Lv, and Shihong Hu. The first draft of the manuscript is written by Yibo Luo and all the authors comment on previous versions of the manuscript. All the authors read and approve the final manuscript.

Acknowledgments

In writing this paper, I have benefited from the presence of my teachers and my classmates. They generously made many invaluable suggestions. I hereby extend my grateful thanks to them for their kind help, without which the paper would not have been what it is.

References

[1] J. R. Giampa, A. S. Bradshaw, and J. A. Schneider, "Influence of dilation angle on drained shallow circular anchor uplift capacity," *International Journal of Geomechanics*, vol. 17, no. 2, article 04016056, 2017.

[2] M. Kanitz, A. Hager, J. Grabe, and C. Goniva, "Numerical and experimental analysis of the extraction mechanism of an anchor plate embedded in saturated sand," *Computers and Geotechnics*, vol. 111, pp. 191–201, 2019.

[3] M. Randolph and S. Gourvenec, *Offshore Geotechnical Engineering*, Spon Press, New York, NY, USA, 2011.

[4] K. Yünkül, Ö. F. Usluoğulları, and A. Gürbüz, "Numerical analysis of geocell reinforced square shallow horizontal plate anchor," *Geotechnical and Geological Engineering*, vol. 39, no. 4, pp. 3081–3099, 2021.

[5] W. Zhong, J. Ouyang, D. Yang, X. Wang, Z. Guo, and K. Hu, "Effect of the in situ leaching solution of ion-absorbed rare earth on the mechanical behavior of basement rock," *Journal of Rock Mechanics and Geotechnical Engineering*, vol. 5, no. 16, pp. 1–22, 2021.

[6] E. A. Dickin, "Uplift behavior of horizontal anchor plates in sand," *Journal of Geotechnical Engineering*, vol. 114, no. 11, pp. 1300–1317, 1988.

[7] K. Ilamparuthi, E. A. Dickin, and K. Muthukrisnaiah, "Experimental investigation of the uplift behaviour of circular plate anchors embedded in sand," *Canadian Geotechnical Journal*, vol. 39, no. 3, pp. 648–664, 2002.

[8] S. P. Singh and S. V. Ramaswamy, "Effect of shape on holding capacity of plate anchors buried in soft soil," *Geomechanics and Geoengineering: An International Journal*, vol. 3, no. 2, pp. 145–154, 2008.

[9] J. Liu, M. Liu, and Z. Zhu, "Sand deformation around an uplift plate anchor," *Journal of Geotechnical and Geoenvironmental Engineering*, vol. 138, no. 6, pp. 728–737, 2012.

[10] J. P. Sahoo and R. Ganesh, "Seismic uplift resistance of circular plate anchors in sand," *Proceedings of the Institution of Civil Engineers-Geotechnical Engineering*, vol. 172, no. 1, pp. 55–66, 2019.

[11] L. H. Zhao, Y. G. Tan, S. H. Hu, D. P. Deng, and X. P. Yang, "Upper bound analysis of ultimate pullout capacity of shallow 3-D circular plate anchors based on nonlinear Mohr-Coulomb failure criterion," *Journal of Central South University*, vol. 25, no. 9, pp. 2272–2288, 2018.

[12] N. Al Hakeem and C. Aubeny, "Numerical investigation of uplift behavior of circular plate anchors in uniform sand," *Journal of Geotechnical and Geoenvironmental Engineering*, vol. 145, no. 9, article 04019039, 2019.

[13] V. N. Khatri and J. Kumar, "Vertical uplift resistance of circular plate anchors in clays under undrained condition," *Computers and Geotechnics*, vol. 36, no. 8, pp. 1352–1359, 2009.

[14] P. Bhattacharya and J. Kumar, "Uplift capacity of anchors in layered sand using finite-element limit analysis: formulation and results," *International Journal of Geomechanics*, vol. 16, no. 3, article 04015078, 2016.

[15] R. S. Merifield, A. V. Lyamin, and S. W. Sloan, "Three-dimensional lower-bound solutions for the stability of plate anchors in sand," *Géotechnique*, vol. 56, no. 2, pp. 123–132, 2006.

[16] D. K. Nguyen, T. P. Nguyen, S. Keawsawasvong, and V. Q. Lai, "Vertical uplift capacity of circular anchors in clay by considering anisotropy and non-homogeneity," *Transportation Infrastructure Geotechnology*, vol. 8, pp. 1–20, 2021.

[17] B. Ukritchon, S. Yoang, and S. Keawsawasvong, "Three-dimensional stability analysis of the collapse pressure on flexible pavements over rectangular trapdoors," *Transportation Geotechnics*, vol. 21, p. 100277, 2019.

[18] B. M. Das and V. K. Puri, "Holding capacity of inclined square plate anchors in clay," *Soils and Foundations*, vol. 29, no. 3, pp. 138–144, 1989.

[19] A. M. Fahmy, J. R. de Bruyn, and T. A. Newson, "Numerical investigation of the inclined pullout behavior of anchors embedded in clay," *Geotechnical and Geological Engineering*, vol. 31, no. 5, pp. 1525–1542, 2013.

[20] R. S. Merifield, A. V. Lyamin, and S. W. Sloan, "Stability of inclined strip anchors in purely cohesive soil," *Journal of Geotechnical and Geoenvironmental Engineering*, vol. 131, no. 6, pp. 792–799, 2005.

[21] P. Bhattacharya and J. Kumar, "Pullout capacity of inclined plate anchors embedded in sand," *Canadian Geotechnical Journal*, vol. 51, no. 11, pp. 1365–1370, 2014.

[22] D. Choudhury and K. S. Subba Rao, "Seismic uplift capacity of inclined strip anchors," *Canadian Geotechnical Journal*, vol. 42, no. 1, pp. 263–271, 2005.

[23] P. Bhattacharya, "Pullout capacity of strip plate anchor in cohesive sloping ground under undrained condition," *Computers and Geotechnics*, vol. 78, pp. 134–143, 2016.

[24] P. Bhattacharya, "Pullout capacity of shallow inclined anchor in anisotropic and nonhomogeneous undrained clay," *Geomechanics & engineering*, vol. 13, no. 5, pp. 825–844, 2017.

[25] R. M. Ramírez-Zamora, M. Solís-López, I. Robles-Gutierrez, Y. Reyes-Vidal, and F. Espejel-Ayala, "A statistical industrial approach for the synthesis conditions of zeolites using fly ash and kaolinite," *Environmental Progress and Sustainable Energy*, vol. 37, no. 1, pp. 318–332, 2018.

[26] J. B. Saedon, N. Jaafar, M. A. Yahaya, N. M. Nor, and H. Husain, "A study on kerf and material removal rate in wire electrical discharge machining of Ti-6Al-4V: multi-objectives optimization," in *2014 2nd International Conference on Technology, Informatics, Management, Engineering & Environment*, Bandung, 2015.

[27] A. Charnley, C. E. Lemke, and O. C. Zienkiewicz, "Virtual work, linear programming and plastic limit analysis," *Proceedings of the Royal Society of London. Series A. Mathematical and Physical Sciences*, vol. 251, no. 1264, pp. 110–116, 1959.

[28] E. Faccioli and E. Vitiello, "A finite element, linear programming methods for the limit analysis of thin plates," *International Journal for Numerical Methods in Engineering*, vol. 5, no. 3, pp. 311–325, 1973.

[29] P. G. Hodge Jr. and T. Belytschko, "Numerical methods for the limit analysis of plates," *Journal of Applied Mechanics, Transactions of the ASME*, vol. 35, no. 4, pp. 796–802, 1968.

[30] A. K. Choudhary, B. Pandit, and G. S. Babu, "Three-dimensional analysis of uplift behaviour of square horizontal anchor plate in frictional soil," *International Journal of Geosynthetics and Ground Engineering*, vol. 4, no. 2, pp. 1–9, 2018.

[31] E. J. Murray and J. D. Geddes, "Uplift of anchor plates in sand," *Journal of Geotechnical Engineering*, vol. 113, no. 3, pp. 202–215, 1987.

[32] R. S. Merifield, A. V. Lyamin, S. W. Sloan, and H. S. Yu, "Three-dimensional lower bound solutions for stability of plate anchors in clay," *Journal of Geotechnical and Geoenvironmental Engineering*, vol. 129, no. 3, pp. 243–253, 2003.

[33] Z. Song, Y. Hu, and M. F. Randolph, "Numerical simulation of vertical pullout of plate anchors in clay," *Journal of Geotechnical and Geoenvironmental Engineering*, vol. 134, no. 6, pp. 866–875, 2008.

[34] L. H. Zhao, Y. G. Tan, Z. H. Nie, X. P. Yang, and S. H. Hu, "Variation analysis of ultimate pullout capacity of shallow horizontal strip anchor plate with 2-layer overlying soil based on nonlinear MC failure criterion," *Journal of Central South University*, vol. 25, no. 11, pp. 2802–2818, 2018.

[35] A. Ghaly and A. Hanna, "Ultimate pullout resistance of single vertical anchors," *Canadian Geotechnical Journal*, vol. 31, no. 5, pp. 661–672, 1994.

[36] D. Wang, Y. Hu, and M. F. Randolph, "Three-dimensional large deformation finite-element analysis of plate anchors in uniform clay," *Journal of Geotechnical and Geoenvironmental Engineering*, vol. 136, no. 2, pp. 355–365, 2010.

[37] R. A. Fisher, "On the probable error of a coefficient of correlation deduced from a small sample," *Metron*, vol. 1, pp. 1–32, 1913.

[38] E. Ostertagová and O. Ostertag, "Methodology and application of oneway ANOVA," *American Journal of Mechanical Engineering*, vol. 1, no. 7, pp. 256–261, 2013.

[39] M. J. Blanca, R. Alarcón, J. Arnau, R. Bono, and R. Bendayan, "Non-normal data: is ANOVA still a valid option?," *Psicothema*, vol. 29, no. 4, pp. 552–557, 2017.